Research Article

# *In Silico* Exploration of the Antimicrobial Potential of *Diospyros*-Derived Bioactives Against *Acinetobacter baumannii*

Soundaryalakshmi Ramesh, Priyanga Paranthaman, Shanthi Veerappapillai and Ramanathan Karuppasamy*
Department of Biotechnology, School of Bio Sciences and Technology, Vellore Institute of Technology, Vellore, Tamil Nadu, India

* Corresponding author. E-mail: kramanathan@vit.ac.in
DOI: 10.14416/j.asep.2026.04.006
Received: 30 September 2025; Revised: 21 November 2025; Accepted: 21 January 2026; Published online: 9 April 2026


**Abstract**
Antimicrobial Resistance (AMR) is a major health threat in the 21st century, driven by the growing number of resistant infections and the lack of new antibiotics. Without effective measures, AMR could become the leading cause of death by 2050. Among the WHO-identified ESKAPE pathogens, *Acinetobacter baumannii* is of particular concern due to its ability to evade antibiotic treatment. Notably, carbapenem-resistant *A. baumannii* (CRAB), driven mainly by overexpression of OXA-23 class D β-lactamase, is associated with prolonged hospital stays and high mortality, making it a top priority for antibiotic research. The lack of effective treatments also increases risks in surgery and chemotherapy. These challenges highlight the need for alternative strategies, with phytochemicals recently gaining attention as promising candidates for combating AMR. Accordingly, a combination of computational pipelines and emerging machine learning–based algorithms was applied to perform a structured investigation of phytochemicals with antibacterial potential. Therefore, this study investigates the potential of the genus *Diospyros* against CRAB, where a total of 448 compounds were retrieved from the Indian Medicinal Plants, Phytochemistry and Therapeutics 2.0 (IMPPAT 2.0) database, of which 135 unique molecules were docked against OXA-23. Machine learning–based scoring refined the results to 20 leads, and ADMET analysis identified Diosindigo B as the most promising candidate with favorable pharmacokinetics, drug-likeness, and low toxicity. The compound was further analyzed using interaction studies, scaffold analysis, and molecular dynamics (MD) simulations. Overall, Diosindigo B shows potential as a therapeutic candidate against CRAB; however, experimental validation is required to confirm its efficacy.

**Keywords:** AMR, *Acinetobacter baumannii*, CRAB, Docking, Diosindigo B, Dynamics

## 1 Introduction

Antimicrobial Resistance (AMR) has become a significant global concern due to the increasing rate of AMR infections and the lack of new antimicrobial treatments [1]. The World Health Organization (WHO) prioritized the ESKAPE pathogens (*Enterococcus faecium*, *Staphylococcus aureus*, *Klebsiella pneumoniae*, *Acinetobacter baumannii*, *Pseudomonas aeruginosa*, and *Enterobacter* species) for new treatments, with *A. baumannii* identified as the most critical due to its exceptional resistance [2]. This Gram-negative bacterium is a major cause of hospital-acquired infections [3], [4]. Its ability to survive harsh conditions and prolonged antibiotic exposure has led to multidrug–resistant (MDR) strains, including resistance to carbapenems, the last–resort treatment option [5]. Carbapenems were once the preferred treatment for MDR *A. baumannii* due to their broad–spectrum activity [2]; however, their frequent use has driven a rise in carbapenem–resistant *A. baumannii* (CRAB), leading the WHO to rank it as the highest priority for antibiotic research and development in 2018 [6], [7]. In 2019, CRAB was implicated in nearly 250,000 of the 1.2 million AMR–related deaths worldwide, underscoring its substantial global health burden [8]. Consequently, a study conducted between 2019 and 2023 investigated the impact of CRAB infections on mortality among intensive care unit (ICU) patients. The findings

revealed that CRAB was the most prevalent pathogen and was associated with markedly higher mortality rates (35% at 14 days, 53% at 28 days, and 74% overall) compared with other Gram-negative bacteria [9]. It is primarily driven by the production of class D β-lactamases, also known as oxacillinases (OXAs), which degrade β–lactam antibiotics. Overexpression of OXA–23 and OXA–51 is linked to carbapenem resistance, with OXA–23 being the most prevalent and clinically significant variant [2].

Phytochemicals have emerged as a promising alternative to combat AMR due to their diverse structures and multitarget antimicrobial effects [10]. Plants produce a wide range of secondary metabolites as part of their defense mechanisms, many of which possess antimicrobial properties and remain integral to traditional medicine practices [11]. Moreover, the structural and functional diversity of plant–derived phytochemicals make them valuable resources for developing new antimicrobial agents [12]. A systematic investigation of such medicinal plants could further lead to the discovery of compounds with unique mechanisms of action. These compounds may act by directly killing bacteria, targeting essential cellular processes, or working synergistically with existing antibiotics to inhibit resistance mechanisms in AMR pathogens [12]. Through these mechanisms, phytochemicals hold the potential to restore antimicrobial efficacy and reverse bacterial resistance. Hence, this study aims to identify phytochemicals with the potential to inhibit AMR in pathogens that require urgent intervention.

Recent research shows that the *Diospyros* genus contains diverse natural compounds, including naphthoquinones, phenolics, terpenoids, and sterols, with strong antibacterial, antifungal, and other biological effects [13]. Because of this chemical richness, *Diospyros* has gained attention as a promising source of agents against MDR pathogens. Notably, isobavacalcione and diospirone from *Diospyros canaliculata* showed strong activity against MDR gram-negative bacteria. Likewise, ursane–type triterpenoids from *Diospyros dendo* leaves exhibited antimicrobial effects against *P. aeruginosa* [13]. In addition, *Diospyros buxifolia* leaf extracts displayed potent antibacterial activity, while stem extracts showed notable antioxidant effects, supporting its role against drug-resistant microbes and oxidative stress [14]. Furthermore, seeds of *Diospyros lotus* demonstrated antimicrobial activity against both gram–positive and gram–negative bacteria, including MDR strains such as *K. pneumoniae*, *A. baumannii*, and *P. aeruginosa* [15]. Overall, these findings suggest that *Diospyros* species may serve as a promising source of novel antimicrobial agents against MDR pathogens.

In recent years, *in silico* approaches have become indispensable tools in drug discovery and development. Advances in computational algorithms, molecular docking, molecular dynamics simulations, and ADMET prediction have greatly enhanced the ability to identify, evaluate, and optimize potential drug candidates efficiently. These methods allow us to predict molecular interactions, binding affinities, and pharmacokinetic properties before experimental testing, thereby reducing both time and cost. Recent studies also demonstrated the growing application of these techniques in identifying novel bioactive compounds with therapeutic potential against a variety of diseases [16]. In view of this, the present study aims to investigate the antimicrobial potential of the plant genus *Diospyros* against CRAB using computational approaches. Phytochemicals from the *Diospyros* genus were screened via molecular docking, ADME and toxicity evaluation, interaction studies, MD simulations, and structural/scaffold analysis to assess their bioactive potential. Overall, this integrative computational strategy provides valuable insights into the bioactive potential of Diospyros–derived phytochemicals and highlights promising candidates that warrant further experimental validation against CRAB.

## 2 Materials and Methods

### 2.1 *Data acquisition*

IMPPAT 2.0 (Indian Medicinal Plants, Phytochemistry and Therapeutics 2.0) is an advanced and comprehensive database that systematically compiles information on Indian medicinal plants, their phytochemicals, and therapeutic applications through extensive manual curation [17]. From this database, the phytochemicals of the genus *Diospyros* were retrieved in both SDF and PDBQT formats.

### 2.2 *Protein and ligand preparation*

The 3D structure of the OXA–23 protein (PDB ID: 4JF4) was obtained from the Protein Data Bank (PDB). Water molecules and other heteroatoms were removed from the protein to ensure accurate protein–ligand docking. Polar hydrogens were added and gasteiger charges were assigned using AutoDockTools

[18]. The processed protein was saved in PDBQT format for docking. The reference compound, meropenem (Pubchem CID: 441130), was retrieved from the PubChem database [19].

### 2.3 *Grid generation*

A grid box was generated around the active site of the target protein to define the docking search space. The active site contains the key residues such as Ser79, Lys82, Leu125, Ser126, Thr217, Trp219, and Arg259, which were used to set the grid parameters [19]. Accordingly, the docking grid was defined as 26 × 26 × 26 points with a spacing of 0.375 Å, centered at x = 10.171, y = -5.071, and z = 4.791. These parameters were saved in a configuration file for docking.

### 2.4 *Molecular docking*

Molecular docking was performed using AutoDock Vina. It is an open–source docking software evolved from AutoDock4 that is used to predict how small molecules bind to target proteins by simulating their interactions and calculating binding affinities. It offers a significant improvement in computational speed and accuracy [20]. The pdbqt files for the protein, ligand, and grid configuration were systematically organized in a directory alongside the Vina application executable. Docking simulations for each ligand, including the reference compound, were performed using Vina. The output file was analyzed, and the best-docked conformation (with the lowest binding affinity) was selected.

### 2.5 *Machine learning–based scoring function*

Recent advancements in machine learning (ML) scoring functions have demonstrated higher accuracy in scoring protein–ligand complexes. These models effectively capture the intricate interactions within protein–ligand systems, making them promising tools for docking applications [21]. With the rapid advancement of ML techniques, ML–based scoring functions often outperform a broad range of traditional scoring functions [22]. Based on these improvements, this study employs two ML–based scoring functions, RF–Score–VS and $K_{DEEP}$, to rescore docking poses, thereby improving the accuracy of binding affinity predictions. The RF score is a numerical value generated by a Random Forest model that predicts the binding affinity of a ligand to a protein in pK units [23]. $K_{DEEP}$ is a 3D convolutional neural network (CNN) model designed for the prediction of binding affinities expressed in kcal/mol. This model is accessible on PlayMolecule.org and is capable of delivering predictions in a matter of seconds [24].

### 2.6 *ADMET analysis*

Pharmacokinetics examines a compound's behavior in the body by assessing ADME (Absorption, Distribution, Metabolism, and Excretion) properties individually. Computational models offer a reliable alternative to experiments for prediction, especially in early-stage drug discovery. In this study, ADME analysis was performed using SwissADME, an online web tool [25]. The lead compounds were evaluated based on various physicochemical, pharmacokinetics, and drug–likeness properties, including molecular weight, rotatable bonds, H–bond acceptors and donors, iLOGP, gastrointestinal (GI) absorption, blood–brain barrier (BBB) permeability, CYP2D6 inhibition, skin permeability (log Kp), Lipinski rule violations, bioavailability, and PAINS alerts. The ProTox 3.0 web server was utilized to predict the toxicity profiles of the lead compounds [26]. Compounds that met the ADME criteria were selected for toxicity assessment, and their toxicity profiles were analyzed using a radar chart.

### 2.7 *Interaction analysis*

The lead compound obtained from the ADMET analysis was further subjected to interaction analysis using LigPlot+ software, which provides insights into hydrogen and hydrophobic bonding between the protein and ligand [27]. The study also assessed whether the bonds were formed with key residues.

### 2.8 *Molecular dynamics simulation*

Molecular dynamics (MD) simulation is a robust approach that provides detailed insights into the structural and dynamic behavior of protein–ligand interactions at the atomic scale [28]. MD simulations were performed for OXA–23 proteins in complex with the reference compound meropenem and the hit compound diosindigo B using GROMACS. Ligand topologies were generated using the CHARMM General Force Field (CGenFF), and protein topologies were prepared with the CHARMM36 force field. Each system was solvated in a dodecahedral Simple Point Charge (SPC) water box and neutralized with counterions. After energy minimization and

equilibration under regulated temperature (NVT) and pressure (NPT) ensembles at 300 K and 1 bar, production MD simulations were run for 50 ns with a 2–fs time step [29]. Trajectories were analyzed for root mean square deviation (RMSD), root mean square fluctuation (RMSF), and hydrogen bond interactions to assess complex stability and flexibility.

## 3 Results and Discussion

### 3.1 *Data acquisition*

AMR represents a major global health challenge, particularly due to the increasing prevalence of multidrug–resistant pathogens. The CRAB, primarily driven by overexpression of OXA–23 β–lactamase, poses significant clinical risks and is prioritized by the WHO for urgent development of new therapeutics. In this regard, phytochemicals offer a promising alternative owing to their structural diversity and multitarget antimicrobial activities. A total of 448 compounds from 16 species of the Genus *Diospyros* were retrieved from the IMPPAT 2.0 database. After removing the duplicates from the initial 448 compounds, a final set of 135 compounds was obtained. These compounds were subjected to docking studies.

### 3.2 *Molecular docking*

Initially, docking analysis was performed to evaluate the binding affinity between the target protein, OXA–23, and the reference compound, Meropenem. Meropenem yielded a docking score of -7.2 kcal/mol. The docked conformation was superimposed onto the corresponding crystal structure to confirm accurate positioning within the binding pocket. The resulting RMSD value of 0.245 Å indicated a close alignment between the docked and crystallographic poses, demonstrating the reliability of the docking protocol (Figure 1). Subsequently, docking was performed for 135 *Diospyros*–derived unique compounds against the target protein. Among these, 71 compounds exhibited more favorable docking scores, ranging from -7.2 to -10.8 kcal/mol, suggesting their potential as stronger binders towards OXA–23.

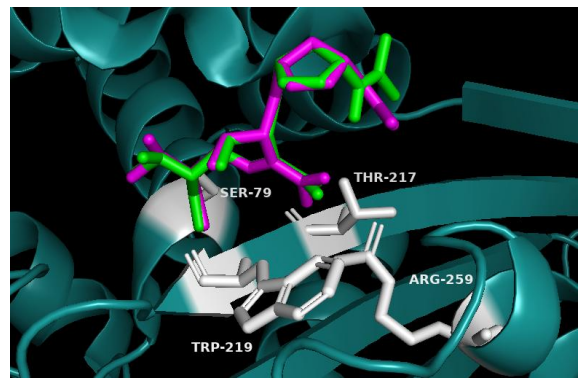


**Figure 1**: Superimposition of re–docked Meropenem (green) and co–crystallized complex (magenta) in the active site of protein OXA–23, highlighting key active site residues (grey).

### 3.3 *Machine learning scoring function*

Machine learning–based scoring approaches were employed to validate the binding affinities of the docked compounds and to ensure greater confidence in selecting the top candidates. Two ML scoring functions, RF–Score–VS and $K_{DEEP}$, were applied to the 71 shortlisted compounds. The reference compound Meropenem yielded an RF–Score of 5.97 and a $K_{DEEP}$ score of -7.49 kcal/mol. The combined use of RF–Score–VS, where higher scores indicate stronger predicted binding, and $K_{DEEP}$, where more negative values reflect tighter binding, provided robust cross–validation of docking outcomes. Notably, 20 compounds achieved better scores than Meropenem in both scoring functions, highlighting the potential of *Diospyros*–derived phytochemicals as promising OXA–23 inhibitors. The detailed scoring results are summarized in Table 1.

### 3.4 *ADMET analysis*

To further evaluate the drug–likeness and safety profile of the shortlisted compounds, ADME analysis was performed for the 20 top–scoring compounds (Table S1). For a compound to qualify as a potential drug candidate, it should have a molecular weight between 150–500 g/mol, no more than 9 rotatable bonds, fewer than 10 hydrogen bond acceptors, and no more than 5 hydrogen bond donors. An iLOGP value of -0.7 to 5.0 ensures solubility and permeability, while favorable features include high GI absorption, no BBB permeability, no CYP2D6 inhibition, a log Kp between -8 and -1, minimal Lipinski's rule violations (0–1), a bioavailability score of 0.55, and a PAINS

score of 0. Among all the screened compounds, only Diosindigo B (IMPHY007947) satisfied all the required parameters for drug–likeness, pharmacokinetics, and physicochemical properties.

**Table 1**: Binding affinity and rescoring results of the reference compound and screened lead compounds against the protein OXA–23.

| S. No | Compound | Affinity (kcal/mol) | Scoring Function | |
|---|---|---|---|---|
| | | | $K_{DEEP}$ (kcal/mol) | RF–Score (pK units) |
| 1 | Meropenem | -7.20 | -7.49 | 5.97 |
| 2 | Diosindigo B (IMPHY007947) | -7.40 | -8.26 | 5.98 |
| 3 | IMPHY012402 | -7.40 | -7.75 | 6.10 |
| 4 | IMPHY011620 | -7.40 | -9.39 | 5.98 |
| 5 | IMPHY014836 | -7.50 | -8.26 | 6.16 |
| 6 | IMPHY012568 | -7.50 | -10.34 | 6.01 |
| 7 | IMPHY011707 | -7.60 | -8.96 | 6.00 |
| 8 | IMPHY004383 | -7.70 | -9.11 | 6.14 |
| 9 | IMPHY015072 | -7.80 | -8.28 | 6.12 |
| 10 | IMPHY014842 | -7.90 | -8.40 | 6.16 |
| 11 | IMPHY014838 | -7.90 | -9.38 | 6.05 |
| 12 | IMPHY002286 | -7.90 | -10.77 | 6.11 |
| 13 | IMPHY011785 | -8.20 | -10.46 | 6.07 |
| 14 | IMPHY004693 | -8.20 | -12.32 | 5.99 |
| 15 | IMPHY008188 | -8.40 | -8.79 | 6.02 |
| 16 | IMPHY013554 | -8.50 | -7.61 | 5.99 |
| 17 | IMPHY004645 | -8.50 | -9.85 | 6.03 |
| 18 | IMPHY012183 | -8.60 | -7.72 | 6.00 |
| 19 | IMPHY008586 | -9.20 | -8.42 | 5.99 |
| 20 | IMPHY005505 | -9.40 | -8.72 | 5.97 |
| 21 | IMPHY014605 | -10.80 | -8.98 | 6.03 |

Toxicity evaluation using the ProTox 3.0 webserver showed that Meropenem (Figure 2(a)) exhibited higher probabilities of nephrotoxicity, respiratory toxicity, clinical toxicity and nutritional toxicity. By comparison, Diosindigo B (Figure 2(b)) displayed a slightly lower toxicity probability across most categories, with only minimal activity in BBB– barrier. In addition, Diosindigo B was classified as toxicity Class 4, indicating no significant toxicity risk.

### 3.5 *Interaction analysis*

The interaction profiling was performed to elucidate the binding mechanisms of the reference and the lead compound within the active site of OXA–23. Although some compounds exhibited more negative docking scores than Diosindigo B, its selection was based on a comprehensive evaluation of both binding affinity and pharmacokinetic suitability, rather than docking score alone. Diosindigo B showed a favorable binding score compared to the reference compound (meropenem), along with supportive RF and $K_{DEEP}$ values. However, ADMET properties are critical in drug discovery, as compounds with strong docking affinities often fail due to poor pharmacokinetics or bioavailability [30]. It is worth mentioning that Diosindigo B was the only compound that satisfied all essential drug–likeness and pharmacokinetic criteria, justifying its selection as the most promising lead candidate. Therefore, the reference compound Meropenem and Diosindigo B were further analyzed for their interactions with the target protein OXA–23 using LigPlot+ software. The active site of OXA–23 comprises Ser79, Lys82, Arg259, Leu125, Lys124, Thr217, Ser126, and Trp219 [19]. Meropenem formed hydrogen bonds with Ser79, Ser126, and Arg259, along with hydrophobic interactions involving Ser79, Trp219, Gly218, Ser126, Arg259, Thr217, Leu125, Lys124, Phe110, Met221, Ala78, and Val128. Among these, the residues Ser79, Lys124, Leu125, Ser126, Thr217, Trp219, and Arg259 are located within the active site of OXA–23, indicating that meropenem interacts with the catalytic pocket. Similarly, Diosindigo B formed hydrogen bonds with Ser126 and Thr217, and hydrophobic interactions with Ala112, Phe110, Trp219, Met221, Gly218, Thr217, Lys124, Ser126, and Leu125. Of these, Ser126, Thr217, Lys124, Leu125, and Trp219 are part of the active–site residues, suggesting that Diosindigo B also binds within the catalytic region of OXA–23. The interaction visuals for both compounds are presented in Figure 3.

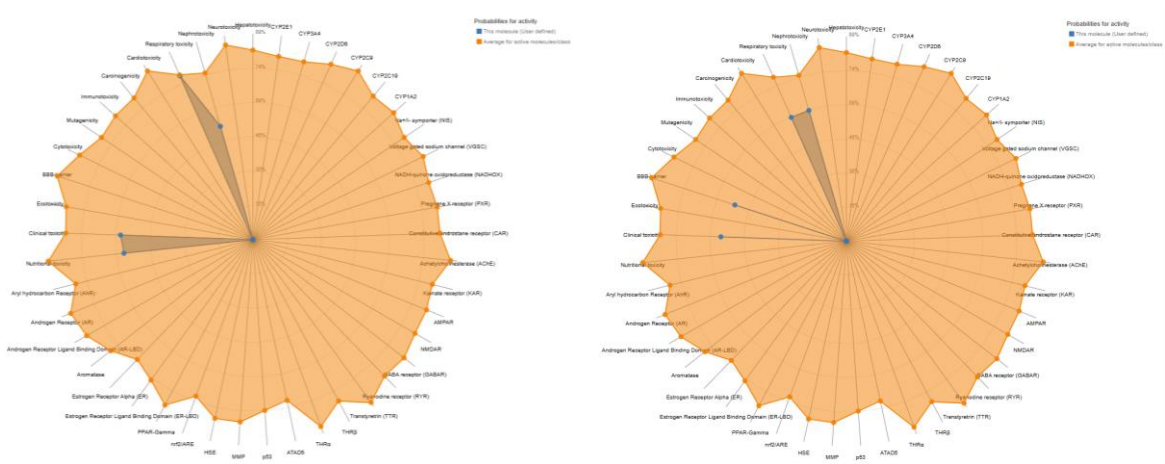

(a) (b)

**Figure 2**: Toxicity radar chart (a) Meropenem (b) Diosindigo B.

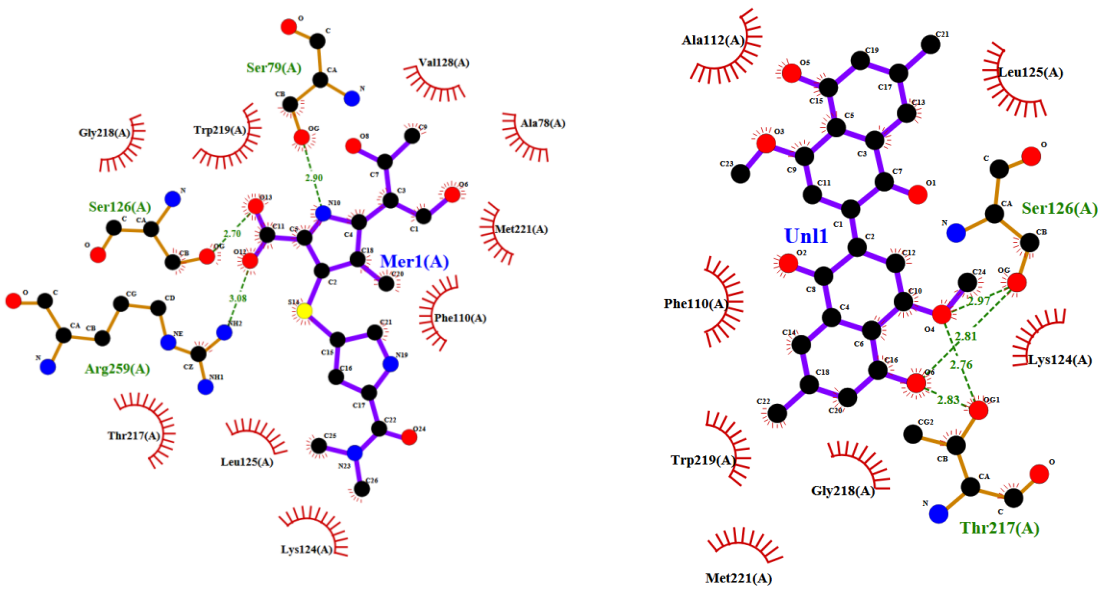


(a) (b)

**Figure 3**: Interaction analysis of (a) Meropenem and (b) Diosindigo B within the catalytic cavity of OXA–23.

### 3.6 *Scaffold analysis*

The scaffold of the selected compound was analyzed via literature to identify key chemical frameworks, functional groups, and substitutions associated with bioactivity. Meropenem is based on a 1–azabicyclo [3.2.0] hept–2–ene system with a β–lactam ring that inhibits bacterial cell wall synthesis by targeting penicillin–binding proteins (Figure 4a). Structural modifications, including a hydroxyethyl group at C6 for β–lactamase stability, a dimethylcarbamoyl pyrrolidine side chain at C2 for broad–spectrum activity, and a carboxyl group for stronger enzyme binding, enhance its action against MDR pathogens [31]. However, it remains vulnerable to degradation by carbapenemases such as OXA–type enzymes, which hydrolyze the β–lactam ring. Diosindigo B, a bis–naphthoquinone derivative composed of two linked naphthoquinone units (Figure 4(b)), exhibits broad–spectrum activity against MDR and ESKAPE

pathogens. Hydroxylated derivatives like Diosindigo B show strong pharmacological potential. Naphthoquinones act through multiple mechanisms, including plasmid curing to remove resistance traits, efflux pump inhibition to enhance antibiotic effectiveness, ROS generation to damage cellular components, and topoisomerase inhibition to exert bacteriostatic effects [32]. These multi–targeted actions highlight Diosindigo B as a promising candidate for combating antimicrobial resistance.

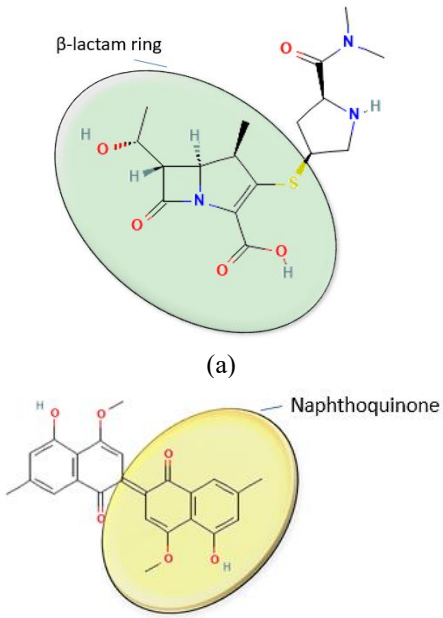


**Figure 4**: Structure of (a) Meropenem, (b) Diosindigo B.

### 3.7 *Molecular dynamics simulation*

MD simulations were performed to assess the stability and flexibility of Meropenem (red) and Diosindigo B (black) within the OXA–23 active site. Key parameters analyzed included RMSD, RMSF, and hydrogen bond interactions. RMSD analysis showed that both complexes exhibited minimal deviation (~0.09–0.10 nm) during the equilibration phase, indicating proper system stabilization (Figure 5). By 20 ns, RMSD increased to ~0.15–0.17 nm for both complexes, reflecting stable conformational changes. Between 20–30 ns, both systems plateaued at ~0.15–0.19 nm. The Diosindigo B complex exhibited slightly fewer fluctuations compared to Meropenem, which showed more local motions. Overall, both complexes remained stable throughout the 50 ns simulation, with Diosindigo B showing slightly lower deviation, suggesting higher overall stability.

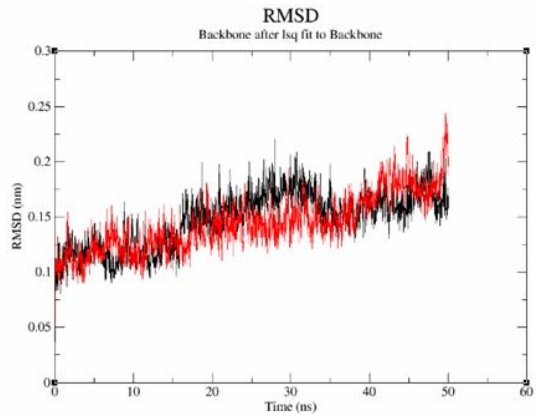


**Figure 5**: Root mean square deviations correspond to the meropenem (red) and diosindigo B (black) complexes throughout the MD simulation.

RMSF analysis revealed higher flexibility in the N–terminal region (residues 25–40), with Meropenem showing a distinct peak near residue 30 (Figure 6). Central regions (residues 40–100 and 120–200) remained relatively stable in both systems, whereas residues 100–120 and 200–250, corresponding to loop regions, displayed greater fluctuations. Meropenem exhibited more pronounced flexibility in these loops compared to Diosindigo B. At the C–terminal region (residues 250–300), both compounds induced moderate fluctuations. Overall, Diosindigo B induced lower residue fluctuations than Meropenem, particularly in loop regions, suggesting reduced local flexibility and more rigid binding.

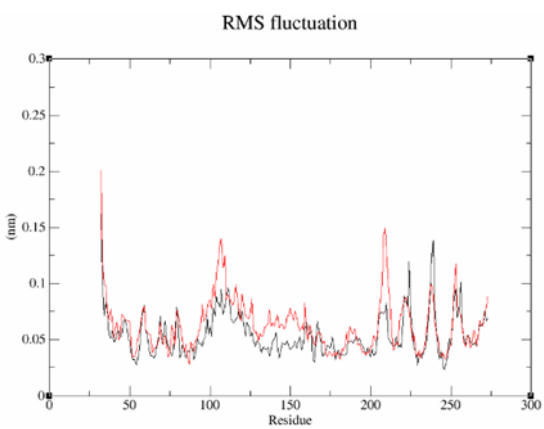


**Figure 6**: RMSF corresponds to the meropenem (red) and diosindigo B (black) complexes throughout the simulation time.

Hydrogen bond analysis showed that Diosindigo B consistently maintained 1–2 hydrogen bonds throughout the simulation (Figure 7). In contrast, Meropenem initially formed ~4 hydrogen bonds, which fluctuated between 0 and 2, with intermittent peaks at 25–30 ns and 40–50 ns reaching 3–5 bonds, indicating fewer stable interactions. Thus, Diosindigo B maintained more consistent hydrogen bonding, whereas Meropenem showed intermittent and weaker interactions, reflecting lower binding persistence.

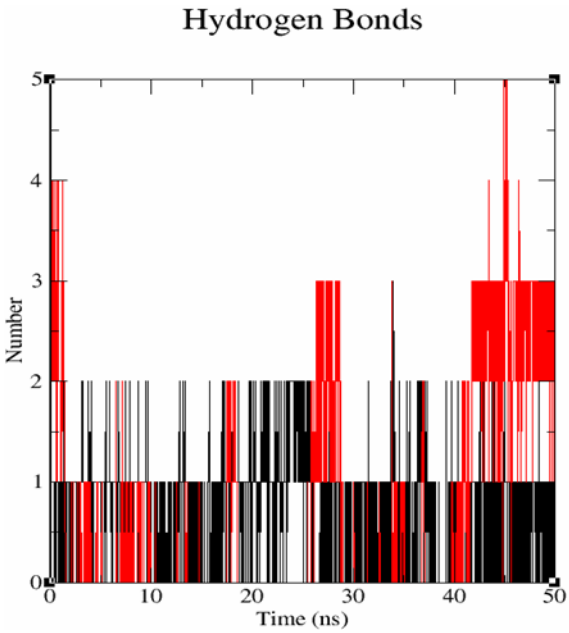


**Figure 7**: Hydrogen Bond observed in protein with other binding residues of meropenem (red) and diosindigo B (black) over the MD simulation.

## 4 Conclusions

This study presents a comprehensive *in silico* investigation to identify natural inhibitors of the carbapenemase enzyme OXA-23, a key driver of CRAB. Out of 448 phytochemicals derived from 16 *Diospyros* species, 135 compounds were docked using AutoDock Vina, of which 71 showed better binding affinity (≤ –7.2 kcal/mol) than the reference drug Meropenem. Refinement with RF-score and $K_{DEEP}$ shortlisted 20 candidates, with Diosindigo B emerging as the most promising due to favorable pharmacokinetic properties and low predicted toxicity. Ligand–protein interaction analysis revealed stable hydrogen bonds and hydrophobic contacts with key residues, while scaffold analysis identified Diosindigo B as a bis-naphthoquinone derivative, a class known for potent antimicrobial effects via plasmid curing, efflux pump inhibition, ROS generation, and DNA topoisomerase inhibition. MD simulations further confirmed Diosindigo B's stable binding, with consistent RMSD, reduced RMSF fluctuations, and persistent hydrogen bonds compared to Meropenem. Together, these results highlight Diosindigo B, from *Diospyros melanoxylon*, as a promising lead compound against carbapenem-resistant *A. baumannii*, though experimental validation remains necessary to confirm its efficacy and safety. The emerging computational techniques and predictive algorithms applied in this study enable efficient structure-based prioritization of natural product leads, accelerating the discovery of potential therapeutics against drug-resistant pathogens. Future studies should aim at experimental validation of the identified compounds through *in vitro* and *in vivo* assays to confirm their antimicrobial activity and safety. Such validation would strengthen the computational findings and provide a foundation for potential therapeutic development.

**Acknowledgements**

The authors thank the management of Vellore Institute of Technology for providing the facilities to carry out this research work.

**Author Contributions**

RK designed the computational framework and analyzed the data. SR and PP performed the computational work and prepared tables and figures. SR, PP, SV, and RK contributed to the writing of the manuscript. RK supervised the entire study. All authors reviewed and approved the manuscript.

**Conflicts of Interest**

The authors declare that they have no conflict of interest.

**Appendix A. Supplementary data**

Supplementary data to this article can be found online here.

**References**


[1] K. W. K. Tang, B. C. Millar, and J. E. Moore, "Antimicrobial resistance (AMR)," *British Journal of Biomedical Science*, vol. 80, p. 11387, 2023.

[2] R. Vázquez-López et al., "*Acinetobacter baumannii* resistance: A real challenge for clinicians," *Antibiotics*, vol. 9, no. 4, p. 205, 2020.

[3] C. Whiteway, A. Breine, C. Philippe, and C. Van der Henst, "*Acinetobacter baumannii*," *Trends in Microbiology*, vol. 30, no. 2, pp. 199–200, 2022.

[4] M. Nguyen and S. G. Joshi, "Carbapenem resistance in *Acinetobacter baumannii*, and their importance in hospital-acquired infections: A scientific review," *Journal of Applied Microbiology*, vol. 131, no. 6, pp. 2715–2738, 2021.

[5] M. Hamidian and S. J. Nigro, "Emergence, molecular mechanisms and global spread of carbapenem-resistant *Acinetobacter baumannii*," *Microbial Genomics*, vol. 5, no. 10, 2019, Art. no. e000306.

[6] S. Ibrahim, N. Al-Saryi, I. M. S. Al-Kadmy, and S. N. Aziz, "Multidrug-resistant *Acinetobacter baumannii* as an emerging concern in hospitals," *Molecular Biology Reports*, vol. 48, no. 10, pp. 6987–6998, 2021.

[7] I. Kyriakidis, E. Vasileiou, Z. D. Pana, and A. Tragiannidis, "*Acinetobacter baumannii* antibiotic resistance mechanisms," *Pathogens*, vol. 10, no. 3, p. 373, 2021.

[8] C. J. Murray et al., "Global burden of bacterial antimicrobial resistance in 2019: A systematic analysis," *The Lancet*, vol. 399, no. 10325, pp. 629–655, 2022.

[9] S. Karakonstantis et al., "Mortality due to carbapenem-resistant *Acinetobacter baumannii* bacteraemia: a 5-year cohort study in intensive care patients," *Clinical Microbiology and Infection*, vol. 31, no. 6, pp. 1033–1039, 2025.

[10] M. V. Ashraf et al., "Phytochemicals as antimicrobials: Prospecting Himalayan medicinal plants as source of alternate medicine to combat antimicrobial resistance," *Pharmaceuticals*, vol. 16, no. 6, p. 881, 2023.

[11] U. Anand, N. Jacobo-Herrera, A. Altemimi, and N. Lakhssassi, "A comprehensive review on medicinal plants as antimicrobial therapeutics: Potential avenues of biocompatible drug discovery," *Metabolites*, vol. 9, no. 11, p. 258, 2019.

[12] N. Vaou et al., "Interactions between medical plant-derived bioactive compounds: Focus on antimicrobial combination effects," *Antibiotics*, vol. 11, p. 1014, 2022.

[13] A. Ribeiro, R. Serrano, I. B. Moreira da Silva, E. T. Gomes, J. F. Pinto, and O. Silva, "The genus *Diospyros*: A review of novel insights into the biological activity and species of Mozambican flora," *Plants*, vol. 12, no. 15, p. 2833, 2023.

[14] N. Fareed, D. M. El-Kersh, F. S. Youssef, and R. M. Labib, "Unveiling major ethnopharmacological aspects of genus *Diospyros* in context to its chemical diversity: A comprehensive overview," *Journal of Food Biochemistry*, vol. 46, 2022, Art. no. e14413.

[15] Z. Akar et al., "RP-HPLC–UV analysis of the phenolic compounds, antimicrobial activity against multidrug-resistant bacteria and antioxidant activity of fruit and seed of *Diospyros lotus* L.," *International Journal of Secondary Metabolite*, vol. 7, no. 4, pp. 237–246, 2020.

[16] S. K. Niazi, Z. Mariam, "Computer-Aided Drug Design and Drug Discovery: A Prospective Analysis," *Pharmaceuticals,* vol. 17, no. 1, p. 22, 2023.

[17] R. P. Vivek-Ananth, K. Mohanraj, A. K. Sahoo, and A. Samal, "IMPPAT 2.0: An enhanced and expanded phytochemical atlas of Indian medicinal plants," *ACS Omega*, vol. 8, no. 9, pp. 8827–8845, 2023.

[18] N. Singh and A. K. Singh, "Phytoconstituents of *Withania somnifera* (L.) Dunal (Ashwagandha) unveiled potential cerebroside sulfotransferase inhibitors: Insight through virtual screening, molecular dynamics, toxicity, and reverse pharmacophore analysis," *Journal of Biological Engineering*, vol. 18, p. 59, 2024.

[19] B. Ramachandran, S. Muthupandian, J. Jeyaraman, and B. S. Lopes, "Computational exploration of molecular flexibility and interaction of meropenem analogs with the active site of oxacillinase-23 in *Acinetobacter baumannii*," *Frontiers in Chemistry*, vol. 11, p. 1090630, 2023.

[20] X. Che, Q. Liu, and L. Zhang, "An accurate and universal protein-small molecule batch docking solution using Autodock Vina," *Results in Engineering*, vol. 19, p. 101335, 2023.

[21] L. Zheng et al., "Improving protein–ligand docking and screening accuracies by incorporating a scoring function correction term," *Briefings in Bioinformatics*, vol. 23, no. 3, 2022, Art. no. bbac051.

[22] C. Shen, J. Ding, Z. Wang, D. Cao, X. Ding, and T. Hou, "From machine learning to deep learning: Advances in scoring functions for protein–ligand docking," *Wiley Interdisciplinary Reviews: Computational Molecular Science*, vol. 10, no. 1, 2019, Art. no. e1429.

[23] M. Wójcikowski, P. J. Ballester, and P. Siedlecki, "Performance of machine-learning scoring functions in structure-based virtual screening," *Scientific Reports*, vol. 7, no. 1, pp. 46710, 2017.

[24] J. Jiménez, M. Škalič, G. Martínez-Rosell, and G. De Fabritiis, "KDEEP: Protein–ligand absolute binding affinity prediction via 3D-convolutional neural networks," *Journal of Chemical Information and Modeling*, vol. 58, no. 2, pp. 287–296, 2018.

[25] A. Daina, O. Michielin, and V. Zoete, "SwissADME: A free web tool to evaluate pharmacokinetics, drug-likeness and medicinal chemistry friendliness of small molecules," *Scientific Reports*, vol. 7, no. 1, pp. 42717, 2017.

[26] P. Banerjee, E. Kemmler, M. Dunkel, and R. Preissner, "ProTox 3.0: A webserver for the prediction of toxicity of chemicals," *Nucleic Acids Research*, vol. *52*, no. W1, pp. W513–W520, 2024.

[27] R. A. Laskowski, and M. B. Swindells. "LigPlot+: multiple ligand-protein interaction diagrams for drug discovery," *Journal of Chemical Information and Modeling*, vol. 51, no. 10, pp. 2778–2786, 2011.

[28] H. Guterres and W. Im, "Improving protein–ligand docking results with high-throughput molecular dynamics simulations," *Journal of Chemical Information and Modeling*, vol. 60, no. 4, pp. 2189–2198, 2020.

[29] P. Paranthaman, R. Karuppasamy, and S. Veerappapillai, "Drug repurposing through biophysical insights: Focus on indoleamine 2,3-dioxygenase and tryptophan 2,3-dioxygenase dual inhibitors," *Cell Biochemistry and Biophysics*, vol. 83, no. 3, pp. 3407–3426, 2025.

[30] P. Murali and R. Karuppasamy, "Exploring the potential of nutraceutical to combat gliomas: Focus on mIDH2 protein," *Frontiers in Physics*, vol. 12, p. 1345834, 2024.

[31] K. M. Papp-Wallace, A. Endimiani, M. A. Taracila, and R. A. Bonomo, "Carbapenems: Past, present, and future," *Antimicrobial Agents and Chemotherapy*, vol. 55, no. 11, pp. 4943–4960, 2011.

[32] N. S. Mone et al., "Naphthoquinones and their derivatives: Emerging trends in combating microbial pathogens," *Coatings*, vol. 11, no. 4, p. 434, 2021.